is zero, it follows that $\nabla\phi_i$ is equal to $\nabla\phi_e$. Hence,

$$J = -(\sigma_i + \sigma_e)\nabla\phi_e = -\sigma\nabla\phi_e. \quad (20)$$

Therefore, the effective conductivity of passive heart muscle is $\sigma_i + \sigma_e$.

What about the abnormal heart? We will identify here several possibly serious difficulties with the inverse problem which arise in the case of pathology.

First of all, $\mu$, the area under the AP, is no longer simply related to the AP duration. Ischemic cells, for example, show a range of changes, including an elevation of resting potential, a decrease in amplitude, a shortening or prolongation of the action potential, and a slower upstroke. Each of these changes affects $\mu$, while a change in resting potential or in amplitude affects $A$. Variation in $A$ means that the inversion of (17) is no longer simply related to $\tau$, but involves the product $A\tau$. Variation in AP waveshape means that $\mu$ obtained from inverting (18) is no longer uniquely associated with a particular AP waveform. Nonetheless, determination of $\mu$ and $A\tau$ might still provide valuable information.

Both $\tau$ and $\mu$ may be expected to vary much less smoothly in the abnormal case. Indeed, an injury may be expected to be confined to one or more limited regions of the heart. Since $\tau$ and $\mu$ are determined only on $S_H$, it may be more difficult to extrapolate to the interior, although knowledge of their values on $S_H$ might well provide sufficient information concerning the injury.

In the case of necrosis, internal surfaces appear. A double layer equal to $\sigma_i\phi_m$ on each such surface then acts as a source in addition to the double layer on the heart surface. A solution to the inverse problem will then yield values of $\tau$ and $\mu$ which are a superposition of their values for the surface cells and an effective value reflecting the internal surfaces. These values on $S_H$ are still unique. If, however, the internal surfaces are unknown (their existence is probably not known), then interpretation of the values of $\tau$ and $\mu$ obtained from the inverse solution becomes more difficult. If an internal necrotic volume is small, it will act approximately as a dipole whose moment is the integral of the double layer over the internal surface.

From (11), the inverse problem could be solved in principle at each instant of time to give $\phi_m$ during the cardiac cycle. The advantage of using integrals of the waveform is that the inverse problem need be solved only twice to provide a complete solution, at least for the normal heart. Furthermore, it may be that the inverse solution for the time integrals is better behaved (less "ill posed") than for $\phi_m$.

Equation (11) also provides at least a strong intuitive explanation for difficulties with the inverse problem. While the inverse solution for $\phi_m$ on $S_H$ is unique, it would appear that ambiguities might easily arise in separating endocardial contributions from epicardial contributions. In other words, since the endocardial and epicardial surfaces are to a considerable extent close and parallel to each other, considerable "crosstalk" might be expected to occur in the influence of sources from opposing regions of the heart surface on body surface potentials.

There are practical difficulties to be considered in evaluating the integrals. For example, accurate determination of the area under *QRS* requires a knowledge of where *QRS* begins and ends. Identification of the end of *QRS* may be difficult in the presence of *ST* segment shifts. Both integrals depend on the accurate determination of the baseline.

## SUMMARY

Consequences of a bidomain model of the heart are explored. The model posits that cardiac sources are proportional to the gradient of the cellular action potential throughout the myocardium. In the absence of necrosis, an equivalent source for the surface electrocardiogram is a double layer on the heart surface whose moment is proportional to the cellular action potential on the surface. The time integral of *QRS* depends on the product of activation time and amplitude of the AP on $S_H$, while the time integral of *QRS-T* depends on the area under the AP on $S_H$. For the normal heart where $A$ is constant, the integral of *QRS* is then directly related to $\tau$, while the integral of *QRS-T* is directly related to AP duration. Solution of the inverse problem would then completely determine $\phi_m$.

In the case of ischemia, the ventricular gradient gives information about $\mu$ which, in turn, depends on the degree of ischemia. The time integral of *QRS* depends on $A\tau$ where $A$ may vary. If the inverse problem can be solved, these parameters will be known on the inner and outer surfaces of the ventricles, thus providing considerable information, albeit ambiguous, about cellular action potentials throughout the ventricular myocardium. The presence of regions of necrosis adds a perturbation to the double layer on $S_H$, and hence to $A\tau$ and $\mu$.

## REFERENCES

[1] W. T. Miller, III, and D. B. Geselowitz, "Simulation studies of the electrocardiogram: I. The normal heart," *Circ. Res.*, vol. 43, pp. 301-315, 1978.

[2] D. B. Geselowitz and W. T. Miller, III, "Active electric properties of cardiac muscle," *Bioelectromagn.*, vol. 3, pp. 127-132, 1982.

[3] D. B. Geselowitz, R. C. Barr, M. S. Spach, and W. T. Miller, III, "The impact of adjacent isotropic fluids on electrograms from anisotropic cardiac muscle," *Circ. Res.*, vol. 51, pp. 602-613, 1982.

[4] W. T. Miller, III, and D. B. Geselowitz, "Simulation studies of the electrocardiogram: II. Ischemia and infarction," *Circ. Res.*, vol. 43, pp. 315-323, 1978.

[5] F. N. Wilson, A. G. MacLeod, P. S. Barker, and F. D. Johnston, "The determination and the significant of the areas of the ventricular deflections of the electrocardiogram," *Amer. Heart J.*, vol. 10, pp. 46-61, 1934.

[6] D. B. Geselowitz, "On bioelectric potentials in an inhomogeneous volume conductor," *Biophys. J.*, vol. 7, pp. 1-11, 1967.

[7] R. McFee and F. D. Johnston, "Electrocardiographic leads: I. Introduction," *Circulation*, vol. 8, pp. 554-568, 1953.

[8] H. Helmholtz, "Uber einege Gesetze der Vertheilung elektrischer Strome in korperlischen Leitern mit Anwendung auf die thierisch elektrischen Versuche," *Pogg. Ann. Bd.*, vol. 89, pp. S211-S213, S353-S357, 1853.

[9] D. B. Geselowitz and W. T. Miller, III, "A bidomain model for anisotropic cardiac muscle," *Ann. Biomed. Eng.*, vol. 11, pp. 191-206, 1983.

[10] J.J.M. Cuppen, "Calculating the isochrones of ventricular depolarization," *SIAM J. Sci. Statist. Comput.*, vol. 5, pp. 105-120, 1984.

[11] A. van Oosterom and J.J.M. Cuppen, "Computing the depolarization sequence at the ventricular surface from body surface potentials" in *Electrocardiology '81, Budapest*, Z. Antaloczy and I. Preda, Eds. Budapest, Hungary: Academic Kiado, 1982, pp. 101-106.

# Muscle Fatigue Monitor (MFM): Second Generation

L. DONALD GILMORE AND CARLO J. DE LUCA

***Abstract*—As a muscular contraction is sustained, the spectrum of the myoelectric signal is shifted toward the lower frequencies. This spectral shift is associated with localized muscular fatigue. This communication describes a computer-assisted device, the Muscle Fatigue Monitor, that performs a quantitative assessment of localized muscular fatigue by tracking changes in the median frequency parameter of the myoelectric signal's spectrum.**

Manuscript received December 29, 1983; revised August 10, 1984. This work was supported in part by the Liberty Mutual Insurance Company.

L. D. Gilmore is with the Liberty Mutual Research Center, Hopkinton, MA 01748.

C. J. De Luca is with the Neuromuscular Research Center and Department of Bioengineering, Boston University, Boston, MA 02215.

0018-9294/85/0100-0075$01.00 

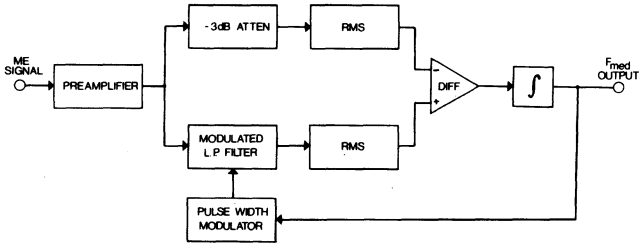


Fig. 1. Block diagram of the signal processing technique used in the first generation muscle fatigue monitor (U.S. Patent 4 213 466).

## INTRODUCTION

Recently, the use of spectral shift of the ME signal as a measure of fatigue is gaining acceptance in the clinical [1]-[3] and the industrial [4]-[7] environments [1]. This spectral shift of the ME signal is associated with the accumulation of metabolic byproducts during a sustained contraction and is a convenient and reliable indicator of fatigue.

In 1981 Stulen and De Luca [9] reported the development of a noninvasive device to calculate the median frequency parameter of the ME power density spectra during fatiguing contractions. They chose the median frequency as the preferred parameter for measuring the spectral shift because it is often a more reliable estimator than other convenient parameters such as mean or mode. A prototype signal processing device to measure median frequency, the muscle fatigue monitor was implemented in analog hardware. The first reports of this implementation appeared in 1978 [10]. U.S. patents were awarded in 1980 [11], [12]. A detailed description of a prototype was published in 1982 [9]. The technique used in the muscle fatigue monitor (MFM) is schematically represented in the block diagram of Fig. 1.

## PRINCIPLES OF OPERATION OF THE FIRST GENERATION MFM

The ME signal is detected with differential surface electrodes and is amplified and filtered to reduce artifacts associated with body movements and high-frequency noise components. The ME signal is passed through a modulated low-pass filter having a sharp rolloff and a circuit that calculates the true rms voltage. This rms voltage is compared to the rms voltage obtained after attenuating the original ME signal by 3 dB and the difference between the two rms values is integrated. The output from the integrator adjusts the cutoff frequency of the low-pass filter so that its output signal amplitude is also attenuated by 3 dB. At this point, the power contained in the signals above and below the cutoff frequency is equal. This is the definition of median frequency. Thus, the integrator output uniquely corresponds to the median frequency of the power spectral density of the ME signal. The evaluation of the first generation prototype MFM device in the laboratory has demonstrated the viability of this analog technique for using spectral shift as an indicator of localized muscular fatigue in clinical and industrial applications [8], [13].

## DESIGN OBJECTIVES OF THE SECOND GENERATION MFM

Based on the experience gained with the laboratory prototype MFM unit, a new portable unit was designed incorporating features useful in clinical and industrial environments. The following criteria were established for the new version of the MFM:

1) four independent analog processing channels and spare data channel,
2) error detection of incorrect ME signal conditions and operator errors,
3) an interactive/prompting display for use by nontechnical personnel,
4) hard copy output of composite graph and text data,
5) audio output proportional to median frequency,
6) presettable initial median frequency (to minimize initial tracking lag),
7) briefcase size portable unit.

To fulfill these varied requirements, a Sharp model PC 1500/CE150 pocket computer/plotter was chosen to control the new device. The use of a small pocket computer offered a simple solution to two main design problems. First, the computer can be programmed to guide the operator through a sequence of events during which the computer controls the analog MFM circuitry. In this way, the MFM becomes its own instruction manual and may be easily used by nontechnical personnel. Second, the computer's integral four-color printer/plotter can produce hard copy of both graphs and text data.

The organization of the new MFM system may be divided into two main sections. The first section describes the modifications and improvements in the analog hardware used to process the median frequency parameter of the ME signal. The second section outlines the implementation of the interface circuitry and the computer software necessary for data acquisition and control of the MFM system.

## ANALOG SIGNAL PROCESSING HARDWARE

Although a microprocessor is incorporated in the new design, the use of real-time digital signal processing techniques utilizing the Sharp computer would be too slow for a multichannel unit. Therefore, an analog signal processing technique similar to the Stulen and De Luca design was chosen. Refer to Fig. 2 for details. The analog signal processing hardware consists of an active surface electrode unit, signal conditioning circuitry, a median frequency tracking loop, and calibration circuitry. The basic signal processing circuit contains several modifications to enhance performance and ensure patient safety.

### *Input Stage with Error Detection*

The architectural arrangement of the detection surfaces within the electrode unit, and the alignment of the detection surfaces with respect to the muscle fiber's orientation, are important considerations in obtaining reliable ME signal spectra. To ensure adequate signal amplitude and bandwidth, yet still retain positioning selectivity, an electrode geometry using two parallel detection surfaces was selected. For a detailed discussion on this subject, refer to the book *Muscles Alive* by Basmajian and De Luca [14]. The detection surfaces consisted of two 1 mm bars of silver wire 1 cm in length, spaced 1 cm apart. The two detection surfaces and a high impedance differential preamplifier were integrated into a small rugged epoxy package. The electrode may be seen in Fig. 3. With this design the electrode/preamp reduces unwanted interference and allows specific electrode placements on small muscles.

The -3 dB bandwidth of the input stage is 20–550 Hz with a filter slope of -12 dB/octave. The 20 Hz cutoff point was selected since the frequency spectrum of the ME signal below 20 Hz is highly variable, reflecting the quasi-random nature of the motor unit discharges. Contribution of low-frequency motion artifacts is also reduced. Interference from signals containing spectral components outside the frequency range of the ME signal is minimized by the 550 Hz low-pass filter. For safety, a medical grade amplifier using a carrier isolation technique electrically isolates the patient from the remaining signal processing circuitry and provides an additional signal gain stage.

To further ensure proper electrode operation throughout a fatigue test, an error detection circuit continuously monitors the signal output from the electrodes. Signal levels above and below a preset amplitude range (±20 $\mu$V to ±4 mV) or signals containing power line induced interference greater than 200 $\mu$V trigger an audible alarm to inform the operator of an error condition.

### *Median Frequency Tracking Loop*

The implementation of the median frequency tracking loop is similar to that of Stulen and De Luca [9], [11], [12] pre-

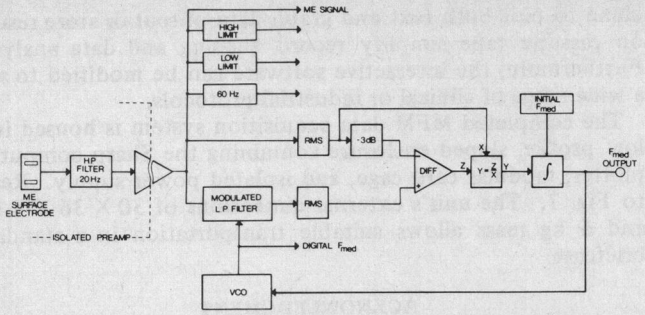


Fig. 2. Block diagram of the signal processing technique used in the second generation muscle fatigue monitor.

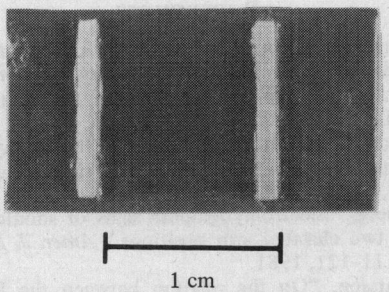


Fig. 3. Molded electrode/preamplifier package used to detect myoelectric activity from the surface of the skin.

viously discussed in the principles of operation of the MFM prototype. Operation of the new design has been enhanced through the use of commercially available switched capacitor filter circuits requiring a minimum of external components and adjustments. The median frequency tracking response has been improved using a circuit which allows the operator to preset the device with an initial median frequency condition. With proper initial frequency selection, accurate estimates of median frequencies can be made during the early stages of a sustained contraction. An additional divider circuit placed after the rms difference amplifier maintains a more consistent loop response time by compensating for variations in signal amplitude over a wide range of input levels.

## Median Frequency Calibration Source

To ensure continued calibration of the analog hardware, an automatic functional check of the median frequency tracking loop is performed by the machine. The calibration circuitry provides a signal source having a known power spectrum and having waveshape and amplitude characteristics similar to signals recorded using surface ME electrodes. The choice of such a signal rather than a single sine wave source allows more accurate determination of any changes in the tracking loop overall frequency response. A median frequency of 100 Hz was selected as the reference value. The calibration circuit was implemented using a bandpass filtered digital white noise source and an analog switched interface controlled by the microcomputer.

The combination of the isolated input preamplifier, signal error detection, and tracking circuit refinements together with calibration circuitry yield a simple analog processing device capable of accurately tracking changes in the median frequency of the ME signal.

## Data/Control Interface Circuitry and Sharp Computer

The new MFM system is configured as a modular data acquisition system consisting of four identical analog signal processing boards communicating with the Sharp computer via a separate communications interface board. (See Fig. 4 for details.) The

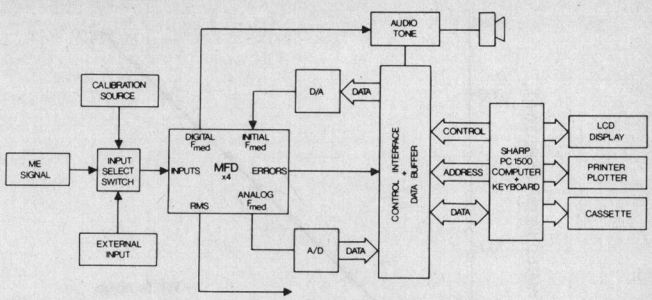


Fig. 4. Block diagram of the second generation muscle fatigue monitor data acquisition system.

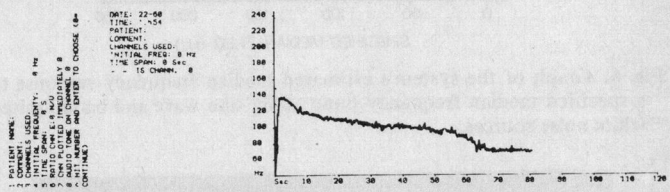

Fig. 5. Sample median frequency graph output generated using the Sharp computer/plotter.

interface circuitry is organized into two sections; data transfer and control, both utilizing a memory mapped architecture. Analog median frequency data from each signal processing board are sampled using a multiplexed 8-channel A/D converter and stored in the computer memory. The four unused A/D inputs can be allocated to sample other experimental parameters such as force, distance, torque, etc. A D/A converter transfers the desired initial median frequency setting to each signal processing board. Error condition outputs from the four signal processing boards are transferred to a 12-bit buffer register and down loaded for computer processing. The remaining control logic of the interface contains address decoding, for the analog and digital converters together with switching circuitry to allow selection of calibration or data inputs and audio tone outputs proportional to median frequency. The control and data bus are terminated in a 40 p-i-n I/O connector for easy access by external devices.

### *Sharp Computer/Plotter*

The versatility of the Sharp computer/plotter allows a multitude of system operating configurations to be selected by software. The standard operating system of the new MFM device consists of a library of subroutines written in Basic language and machine code. These subroutines handle data acquisition and control of each analog signal processing card, the LCD dot matrix display, and printer/plotter output. The appropriate combination of these subroutines allows the user to tailor the system programming to his individual needs. These programs may be stored in memory or on cassette tape giving the new MFM device additional flexibility. In a typical clinical application, the device is programmed to store and print information about the patient and particular test protocol. The device then guides the operator throughout the duration of the test storing data in memory while continually monitoring the system for error conditions. At the successful completion of a test, the stored data are plotted in a four-color graph along with time, date, and patient information. A sample output is presented in Fig. 5. Test data may also be stored on cassette tape and retrieved by the computer at a later date for an evaluation of the patient's progress.

## Evaluation of the Second Generation MFM

The new MFM has been evaluated in the area of circuit performance and interactive operation.

The ability of the device to accurately track the median frequency of a signal was measured using ME signals, sine waves,

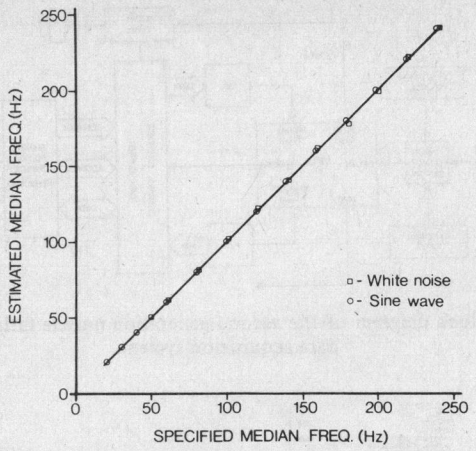


Fig. 6. Graph of the system's estimated median frequency response to a specified median frequency input using sine wave and band-limited white noise sources.

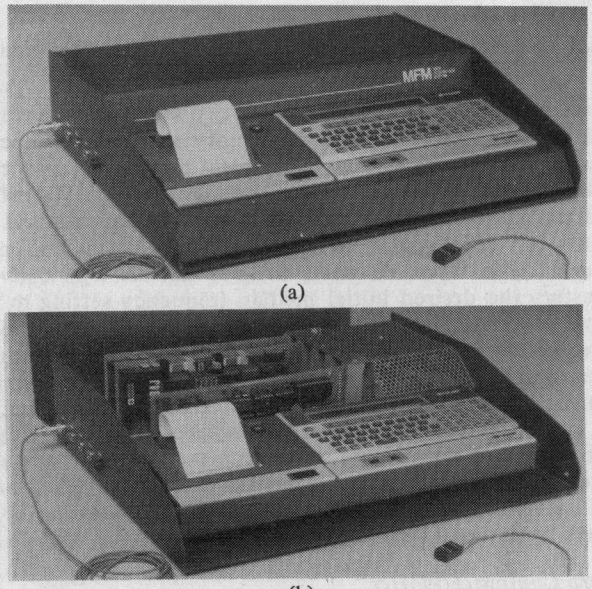

(a)

(b)

Fig. 7 (a) and (b) MFM data acquisition system package.

and band-limited white noise sources having known power density spectral shifts. These results compared favorably to those obtained using digitally computed FFT spectral analysis algorithms, showing a deviation of less than 5 percent within a range of median frequencies from 20–255 Hz. Refer to Fig. 6. The smoothing time constant of the analog tracking loop was chosen to be 0.5 s for these tests. However, other loop time constants can be selected to optimize system performance for other conditions. Shorter time constants would be useful for exhausting contractions of short duration during which the median frequency changes rapidly. Longer time constants could be selected to observe trends in periodic contractions.

The error detection circuitry incorporated into the device reliably indicated the presence of any faults occurring at the electrode interface. Poor electrode contact with the skin, excessive power line interference (typically 60 Hz components with amplitudes greater than 200 $\mu$V at the recording contacts), or low ME signal amplitudes were easily detected and appropriate warning signals displayed to the operator. One of the salient features of the new device is its ability to interact with the operator via the visual display, audio tone generator, and keyboard. The reliability of the test data is increased since there is less chance for operator error. The ability of the machine to plot both text and graph data output or store results on cassette tape simplify record keeping and data analysis. Furthermore, the interactive software can be modified to suit a wide range of clinical or industrial protocols.

The completed MFM data acquisition system is housed in a low profile, sloped enclosure containing the Sharp computer/plotter, modular card cage, and isolated power supply. Refer to Fig. 7. The unit's external dimensions of 30 X 36 X 8 cm and 6 kg mass allows suitable transportation in a standard briefcase.

## ACKNOWLEDGMENT

The authors would like to express their gratitude to W. M. Enzing for his valuable contribution to the design of the MFM data acquisition system.

## REFERENCES

[1] H. Broman, R. Magnusson, I. Petersen, and R. Ortengren, "Vocational electromyography," in *New Developments in EMG and Clinical Neurophysiology*, vol. 1, J. E. Desmedt, Ed. 1973, pp. 656–664.

[2] I. Peterson, R. Kadefors, and J. Person, "Neurophysiologic studies of welders in shipbuilding work," *Environ. Res.*, vol. 11, pp. 226–236, 1976.

[3] M. Hagberg, "Electromyographic signs of shoulder muscular fatigue in two elevated arm positions," *Amer. J. Phys. Med.*, vol. 60, pp. 111–121, 1981.

[4] L.-E. Larsson, "On the relation between the EMG frequency spectrum and the duration of symptoms in lesions of the peripheral motor neuron," *Electroencephalogr. Clin. Neurophysiol.*, vol. 38, pp. 69–78, 1975.

[5] T. W. Schweitzer, J. W. Fitzgerald, J. A. Bowden, and P. Lynne-Davies, "Spectral analysis of human inspiratory diaphragmatic electromyograms," *J. Appl. Physiol.*, vol. 46, pp. 152–165, 1979.

[6] H. W. Ladd, H. Broman, and M. D. O'Riain, "Regenerative processes in peripheral nerve injury: A new method for their evaluation," *Arch. Phys. Med. Rehab.*, vol. 63, pp. 124–129, 1982.

[7] F. Bellemare and A. Grassino, "Evaluation of human diaphragm fatigue," *J. Appl. Physiol.*, vol. 53, pp. 1196–1206, 1982.

[8] C. J. De Luca, "Myoelectric manifestations of localized muscular fatigue in humans," in *CRC, Critical Reviews in Bioengineering*, to be published.

[9] F. B. Stulen and C. J. De Luca, "Muscle fatigue monitor: A noninvasive device for observing localized muscular fatigue," *IEEE Trans. Biomed. Eng.*, vol. BME-29, pp. 760–769, Dec. 1982.

[10] ——, "A noninvasive device for monitoring metabolic correlates of myoelectric signals," in *Proc. 31st Ann. Conf. Eng. Med. Biol.*, vol. 264, 1978.

[11] ——, "Monitoring myoelectric signals," July 22, 1980, U.S. Patent 4 213 467.

[12] F. B. Stulen, "Monitoring myoelectric signals," July 22, 1980, U.S. Patent 4 213 466.

[13] C. J. De Luca, M. A. Sabbahi, F. B. Stulen, and G. Bilotto, "Some properties of the median frequency of the myoelectric signal during localized muscle fatigue," in *Biochemistry of Exercise*, vol. 13, H. K. Knuttgen, J. A. Vogel, and J. Poortmans, Eds. 1983, pp. 175–186.

[14] J. V. Basmanan and C. J. De Luca, *Muscles Alive*, 5th ed. Baltimore, MD: Williams and Wilkins, 1984.

## Analysis of a Digital EMG Signal Processor in Dynamic Conditions

T. D'ALESSIO

*Abstract*—**The performances of digital electromyographic signal processors in dynamic conditions are determined by evaluating the root-**

Manuscript received January 3, 1984; revised August 3, 1984.

The author is with the Dipartimento di Scienza e Tecnica dell'Informazione e della Comunicazione, Università di Roma, 00184 Rome, Italy.